JOC Article

Tuning the HOMO and LUMO Energy Levels of Organic Chromophores for Dye Sensitized Solar Cells

Daniel P. Hagberg,[†] Tannia Marinado,[‡] Karl Martin Karlsson,[†] Kazuteru Nonomura,[‡] Peng Qin,[†] Gerrit Boschloo,[‡] Tore Brinck,[‡] Anders Hagfeldt,*[,‡] and Licheng Sun*[,†]

Organic Chemistry, Center of Molecular Devices, Department of Chemistry, KTH Chemical Science and Engineering, 10044 Stockholm, Sweden, and Physical Chemistry, Center of Molecular Devices, Department of Chemistry, KTH Chemical Science and Engineering, 10044 Stockholm, Sweden

lichengs@kth.se; hagfeldt@kth.se

Received July 28, 2007

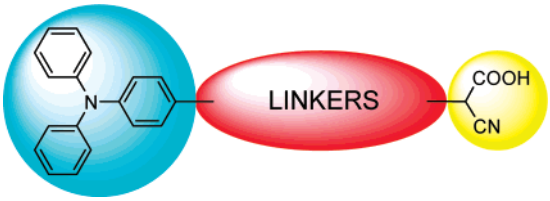

A series of organic chromophores have been synthesized in order to approach optimal energy level composition in the TiO_2−dye−iodide/triiodide system in the dye-sensitized solar cells. HOMO and LUMO energy level tuning is achieved by varying the conjugation between the triphenylamine donor and the cyanoacetic acid acceptor. This is supported by spectral and electrochemical experiments and TDDFT calculations. These results show that energetic tuning of the chromophores was successful and fulfilled the thermodynamic criteria for dye-sensitized solar cells, electrical losses depending on the size and orientation of the chromophores were observed.

Introduction

Organic chromophores for the dye-sensitized solar cell (DSSC), the so-called Grätzel cell,[1] have drawn the attention of many research groups in the last couple of years. In comparison, the conventional ruthenium-based sensitizers such as the **N3**/**N719**[2,3] and the black dye[4] have been intensively investigated and show record solar-energy-to-electricity conversion efficiencies of 11% under AM 1.5 irradiation, while the organic sensitizers have reached efficiencies in the range of 5−8%.[5−12]

Organic chromophores have certain advantages over ruthenium-based sensitizers. They exhibit high molar extinction coefficients and are easily modified due to short synthetic routes. The high extinction coefficients of the organic dyes are suitable for the thin TiO_2 films required in solid-state devices where mass transport and insufficient pore filling limit the photovoltaic performance.[13]

[†] Organic Chemistry.
[‡] Physical Chemistry.

(1) O'Regan, B.; Gratzel, M. *Nature* **1991**, *353*, 737.
(2) Nazeeruddin, M. K.; Kay, A.; Rodicio, I.; Humphry-Baker, R.; Muller, E.; Liska, P.; Vlachopoulos, N.; Gratzel, M. *J. Am. Chem. Soc.* **1993**, *115*, 6382.
(3) Nazeeruddin, M. K.; Zakeeruddin, S. M.; Humphry-Baker, R.; Jirousek, M.; Liska, P.; Vlachopoulos, N.; Shklover, V.; Fisher, C. H.; Gratzel, M. *Inorg. Chem.* **1999**, *38*, 6298.
(4) Nazeeruddin, M. K.; Pechy, P.; Renouard, T.; Zakeeruddin, S. M.; Humphry-Baker, R.; Comte, P.; Liska, P.; Cevey, L.; Costa, E.; Shklover, V.; Spiccia, L.; Deacon, G. B.; Bignozzi, C. A.; Gratzel, M. *J. Am. Chem. Soc.* **2001**, *123*, 1613.
(5) Hara, K.; Sato, T.; Katoh, R.; Furube, A.; Ohga, Y.; Shinpo, A.; Suga, S.; Sayama, K.; Sugihara, H.; Arakawa, H. *J. Phys. Chem. B* **2003**, *107*, 597.
(6) Horiuchi, T.; Miura, H.; Sumioka, K.; Uchida, S. *J. Am. Chem. Soc.* **2004**, *126*, 12218.
(7) Hara, K.; Sato, T.; Katoh, R.; Furube, A.; Yoshihara, T.; Murai, M.; Kurashige, M.; Ito, S.; Shinpo, A.; Suga, S.; Arakawa, H. *Adv. Funct. Mater.* **2005**, *15*, 246.
(8) (a) Hagberg, D. P.; Edvinsson, T.; Marinado, T.; Boschloo, G.; Hagfeldt, A.; Sun, L. *Chem. Commun.* **2006**, 2245. (b) Tian, H.; Yang, X.; Chen, R.; Pan, Y.; Li, L.; Hagfeldt, A.; Sun, L. *Chem. Commun.* **2007**, 3741. (c) Chen, R.; Yang, X.; Tian, H.; Wang, X.; Hagfeldt, A.; Sun, L. *Chem. Mater.* **2007**, *19*, 4007−4015.
(9) Koumura, N.; Wang, Z. S.; Mori, S.; Miyashita, M.; Suzuki, E.; Hara, K. *J. Am. Chem. Soc.* **2006**, *128*, 14256.
(10) Kim, S.; Lee, J. K.; Kang, S. O.; Ko, J.; Yum, J. H.; Fantacci, S.; De Angelis, F.; Di Censo, D.; Nazeeruddin, M. K.; Gratzel, M. *J. Am. Chem. Soc.* **2006**, *128*, 16701.
(11) Wang, Z. S.; Cui, Y.; Hara, K.; Dan-oh, Y.; Kasada, C.; Shinpo, A. *Adv. Mater.* **2007**, *19*, 1138.
(12) Kitamura, T.; Ikeda, M.; Shigaki, K.; Inoue, T.; Andersson, N. A.; Ai, X.; Lian, T.; Yanagida, S. *Chem. Mater.* **2004**, *16*, 1806.

10.1021/jo701592x CCC: $37.00
Published on Web 11/03/2007

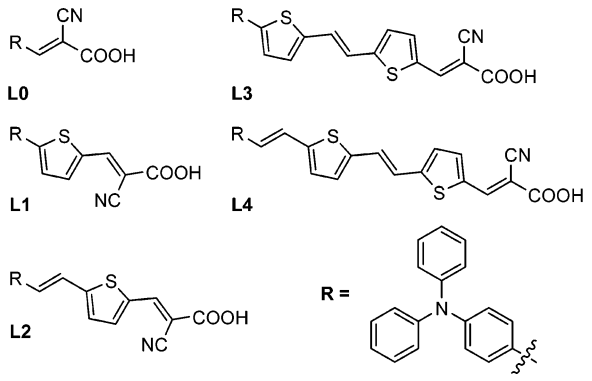

FIGURE 1. Structures of the chromophores.

The efficiencies of the sensitizers are related to some basic criteria.[10] The HOMO potential of the dye should be sufficiently positive compared to the electrolyte redox potential for efficient dye regeneration.[14] The LUMO potential of the dye should be sufficiently negative to match the potential of the conduction band edge of the TiO_2 and its orbitals should be located at the acceptor part of the dye to provide efficient electron injection. Excitation by light should induce an intramolecular charge separation of the donor and acceptor moieties of the chromophore, i.e., a pronounced push−pull effect.

Recently, we published the synthesis and characterization of an organic dye (**L2**) that gave total solar-to-energy conversion efficiency of 5%, in comparison with the conventional **N719**, which gave 6% under the same conditions.[8,15] To extend the spectral response of this chromophore toward the red region and to fine-tune the HOMO and the LUMO energy levels of the sensitizer a series of dyes was designed, see Figure 1. The chromophores consist of donor, linker, and acceptor groups. By alternating the different groups independently, we can systematically record the contributions of different groups and attain a HOMO and LUMO energy library. This screening strategy helps us to optimize the TiO_2−dye−iodide/triiodide system in terms of balance between photovoltage, driving forces, and spectral response for future preparation of highly efficient dyes by matching suitable donor−linker−acceptor components. In addition, the compatibility of novel dyes and future semiconductor−redox systems could more easily be investigated by using an already existing HOMO and LUMO energy library. In this series of dyes, the π-conjugated systems between the donor (triphenylamine moiety) and the acceptor (cyanoacetic acid moiety) were systematically extended to adjust the molecular HOMO and LUMO energy levels of the dyes, hence red-shifting and broadening the absorption spectra with the number of π-conjugations introduced. By introducing thiophene to extend the number of π-conjugations the stability of the chromophores is less affected than that of polyene linkers.[16] The dyes were designed for future solid state applications with triarylamine-based hole conductors in mind and for this reason thinner films (3 μm) were used to demonstrate the advantage of chromophores with higher extinction coefficients.

Results and Discussion

The synthetic strategy, illustrated in Scheme 1, involves the Suzuki coupling reaction[17] (**L1**) and/or the Wittig reaction[18,19] (**L2**, **L3**, and **L4**) to extend the thiophene linker. The Suzuki coupling reaction was made with unprotected 5-formyl-2-thiophene-boronic acid and 4-(diphenylamino)bromobenzene under microwave irradiation to directly yield the aldehyde necessary for further reactions.[20] In the cases of linker extension by the Wittig reaction, formylation of the thiophene with *n*-BuLi and DMF was applied. Both the cis and the trans isomers were formed, hence cis-to-trans isomerization by I_2 was necessary to obtain the pure trans-conformation of the target compounds which possess better photostability properties.[21] The final reaction for all five dyes was condensation of the respective aldehyde with cyanoacetic acid by the Knoevenagel reaction in the presence of piperidine.

Table 1 presents the experimental spectral and electrochemical properties of the dyes in acetonitrile solution and adsorbed onto TiO_2. A systematic red-shift in the absorption maximum with increasing conjugation was observed for deprotonated dye solutions (Figure 2, left); deprotonation was achieved by adding TBAOH to the dye solutions. In contrast the spectra of the dyes in plain acetonitrile (shown in Figure 2, inset) displayed no clear correlation to the conjugation structure, indicating a different degree of protonation for the dyes in the solvent acetonitrile. Upon adsorption onto TiO_2 the dye spectra are broadened (Figure 2, right), and the absorption shoulder on the low-energy side was extended with increased linker conjugation. This is an advantageous spectral property for light harvesting of the solar spectrum. The emission spectra also showed an equivalent red-shift upon increased linker conjugation (see Table 1).

The oxidation potentials of the dyes in acetonitrile were determined by differential pulse voltammetry, and are listed in Table 1. Increased linker conjugation length resulted in less positive oxidation potentials. The estimated LUMO potentials calculated from ($E_{ox} - E_{0-0}$) are sufficiently more negative than the TiO_2 CB edge for all five dyes, as reported in Table 1.

We have computed equilibrium structures for the four dyes using density functional theory (DFT) at the B3LYP/MIDI! level. The lowest excited states were characterized by time-dependent DFT (TDDFT) at the same level. All calculations were performed with the Gaussian 03 software.[22] The ground state geometries are completely planar except for the amino group, which have the phenyl groups rotated to avoid sterical clashes. It can be noted that in dyes **L1** and **L3** the planarity results in short distances of 2.2 Å between hydrogens on phenyl and thiophene groups that are adjacent. Semiempirical AM1 calculations give slightly twisted structures due to these interactions, but the B3LYP calculations result in a planar linker chain. The TDDFT calculations show that in all five dyes the lowest excitation is a charge-transfer transition of dominantly HOMO−

(13) Schmidt-Mende, L.; Bach, U.; Humphry-Baker, R.; Horiuchi, T.; Miura, H.; Ito, S.; Uchida, S.; Gratzel, M. *Adv. Mater.* **2005**, *17*, 813.
(14) Qin, P.; Yang, X.; Chen, R.; Sun, L. C.; Marinado, T.; Edvinsson, T.; Boschloo, G.; Hagfeldt, A. *J. Phys. Chem. C* **2007**, *111*, 1853.
(15) Johansson, E. M. J.; Edvinsson, T.; Odelius, M.; Hagberg, D. P.; Sun, L. C.; Hagfeldt, A.; Siegbahn, H.; Rensmo, H. *J. Phys. Chem. C* **2007**, *111*, 8580.
(16) Hara, K.; Kurashige, M.; Dan-oh, Y.; Kasada, C.; Shinpo, A.; Suga, S.; Sayama, K.; Arakawa, H. *New J. Chem.* **2003**, *27*, 783.
(17) Suzuki, A. *J. Organomet. Chem.* **1999**, *576*, 147.
(18) Wittig, G. *J. Organomet. Chem.* **1975**, *100*, 279.
(19) Hu, Z. Y.; Fort, A.; Barzoukas, M.; Jen, A. K. Y.; Barlow, S.; Marder, S. R. *J. Phys. Chem. B* **2004**, *108*, 8626.
(20) Melucci, M.; Barbarella, G.; Zambianchi, M.; Di Pietro, P.; Bongini, A. *J. Org. Chem.* **2004**, *69*, 4821.
(21) Lequan, M.; Lequan, R. M.; Chane-Ching, K.; Callier, A. C. *Adv. Mater. Opt. Electron.* **1992**, *1*, 243.

SCHEME 1. Synthesis of the Chromophores

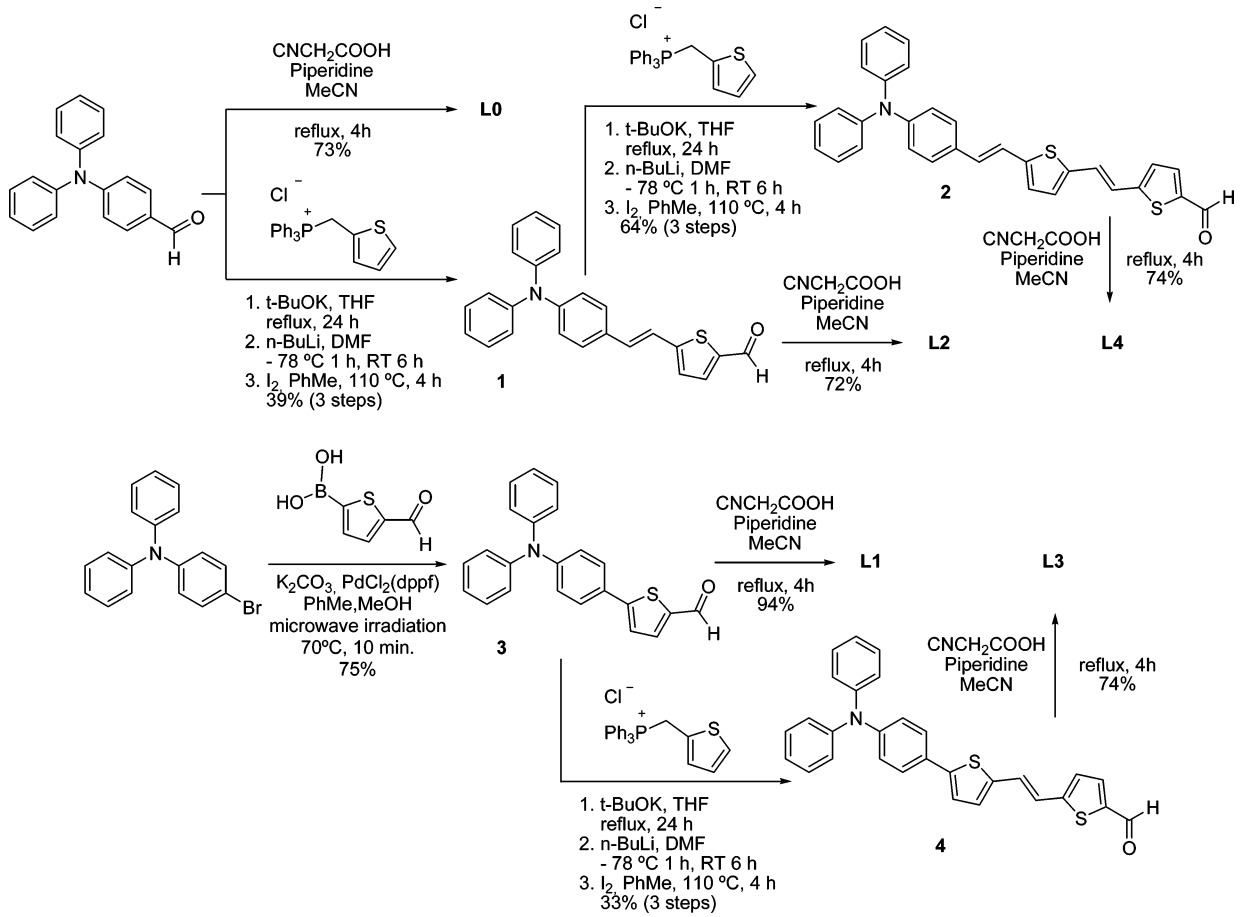

TABLE 1. Experimental Data for Spectral and Electrochemical Properties of the Dyes

dye	Abs_{max} [nm][a]	ϵ [M^{-1} cm^{-1}][b]	E_{max} [nm][c]	E(ox) [V] vs NHE[d]	E_{0-0} [eV][e]	E_{LUMO} [V] vs NHE[f]
L0[g]	373,[i] 387[ii]	36 000	509	1.37	2.90	−1.53
L1	404,[i] 404[ii]	25 000	548	1.21	2.64	−1.43
L2	427,[i] 409[ii]	38 000	594	1.13	2.48	−1.36
L3	445,[i] 412[ii]	49 000	621	1.07	2.38	−1.32
L4	463,[i] 415[ii]	62 000	644	1.01	2.35	−1.34

[a] Absorption of the deprotonated dyes in MeCN solution[i] and adsorbed onto TiO_2[ii]. [b] Extinction coefficients determined in THF solution. [c] Emission maximum of the deprotonated dyes in acetonitrile, excited at absorption maximum. [d] The ground state oxidation potential (first oxidation peak) of the dyes were measured with differential pulse voltammetry, DVP, under the following conditions: 0.1 M tetrabutylammonium hexafluorophosphate, TBA(PF_6) in acetonitrile, a Pt working electrode, a silver counter electrode and the reference electrode was a silver wire calibrated with ferrocene/ferrocenium (Fc/Fc^+) as an internal reference. [e] The 0−0 transition energy is estimated from the intersection of normalized absorption and emission curves from solution measurements. [f] The estimated LUMO position from addition of the estimated 0−0 transition energy to the ground state oxidation potential vs NHE. [g] Previously studied by Kitamura et al.[12]

LUMO character. Computed HOMO and LUMO orbitals of the dyes **L1** and **L4** are depicted in Figure 3. As indicated by the figure, the general characters of the orbitals are independent of the linker length. The HOMO orbital is of π-character and is delocalized over the entire molecule, including the phenyl groups of the amino nitrogen, which further supports the dependence of the HOMO potentials observed in electrochemical experiments. In the LUMO-orbital, which also has π-character, there is essentially no contribution from the amino phenyl groups, and the electron density has been shifted toward the other end of the molecule. This indicates that the dipole moment should be considerably larger in the first excited state compared to the ground state. Consequently, the computed oscillator strength is large in all molecules, and it increases with the length of the linker (Table 2). Also the absorption wavelength increases with linker length in agreement with experimental absorption spectra. However, the computed wavelengths are overestimated, and the overestimation is more pronounced for the longer dyes. This is expected since traditional exchange-correlation functionals, such as B3LYP, underestimate the energies for charge-transfer transitions and the error increases with the distance between the negative and positive charges of the charge-transfer state.[23]

Solar cell performance of the dyes was tested by using thin TiO_2 films (∼3 μm). The spectra of monochromatic incident

(22) Frisch, M. J.; Trucks, G. W.; Schlegel, H. B.; Scuseria, G. E.; Robb, M. A.; Cheeseman, J. R.; Montgomery, J. A., Jr.; Vreven, T.; Kudin, K. N.; Burant, J. C.; Millam, J. M.; Iyengar, S. S.; Tomasi, J.; Barone, V.; Mennucci, B.; Cossi, M.; Scalmani, G.; Rega, N.; Petersson, G. A.; Nakatsuji, H.; Hada, M.; Ehara, M.; Toyota, K.; Fukuda, R.; Hasegawa, J.; Ishida, M.; Nakajima, T.; Honda, Y.; Kitao, O.; Nakai, H.; Klene, M.; Li, X.; Knox, J. E.; Hratchian, H. P.; Cross, J. B.; Adamo, C.; Jaramillo, J.; Gomperts, R.; Stratmann, R. E.; Yazyev, O.; Austin, A. J.; Cammi, R.; Pomelli, C.; Ochterski, J. W.; Ayala, P. Y.; Morokuma, K.; Voth, G. A.; Salvador, P.; Dannenberg, J. J.; Zakrzewski, V. G.; Dapprich, S.; Daniels, A. D.; Strain, M. C.; Farkas, O.; Malick, D. K.; Rabuck, A. D.; Raghavachari, K.; Foresman, J. B.; Ortiz, J. V.; Cui, Q.; Baboul, A. G.; Clifford, S.; Cioslowski, J.; Stefanov, B. B.; Liu, G.; Liashenko, A.; Piskorz, P.; Komaromi, I.; Martin, R. L.; Fox, D. J.; Keith, T.; Al-Laham, M. A.; Peng, C. Y.; Nanayakkara, A.; Challacombe, M.; Gill, P. M. W.; Johnson, B.; Chen, W.; Wong, M. W.; Gonzalez, C.; Pople, J. A. *Gaussian 03*; Gaussian, Inc.: Pittsburgh, PA, 2003.

(23) Dreuw, A.; Head-Gordon, M. *Chem. Rev.* **2005**, *105*, 4009.

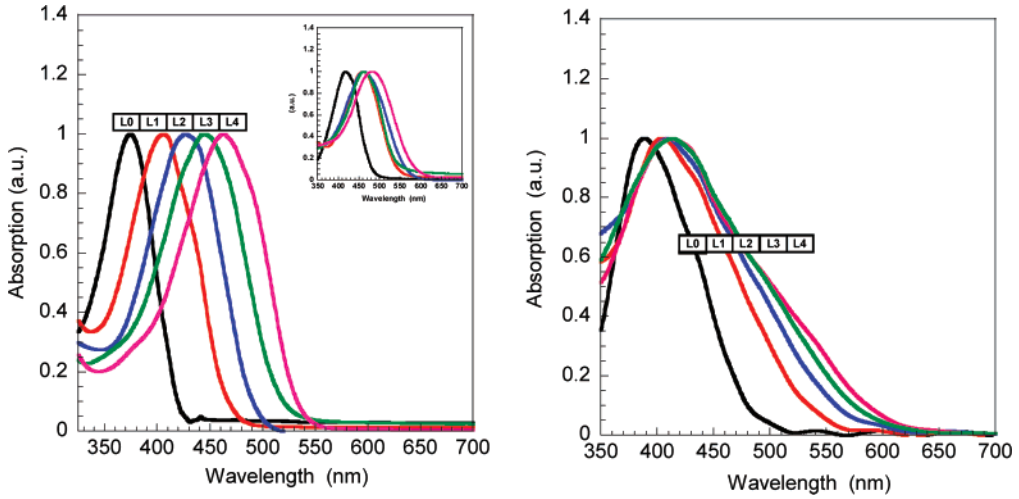

FIGURE 2. (Left) Normalized absorption spectra of the **L0**−**L4** dyes in acetonitrile solution upon addition of TBAOH. Inset: Normalized absorption spectra of the **L0**−**L4** dyes in a plain acetonitrile solution. (Right) Normalized absorption spectra of the **L0**−**L4** dyes adsorbed onto TiO_2.

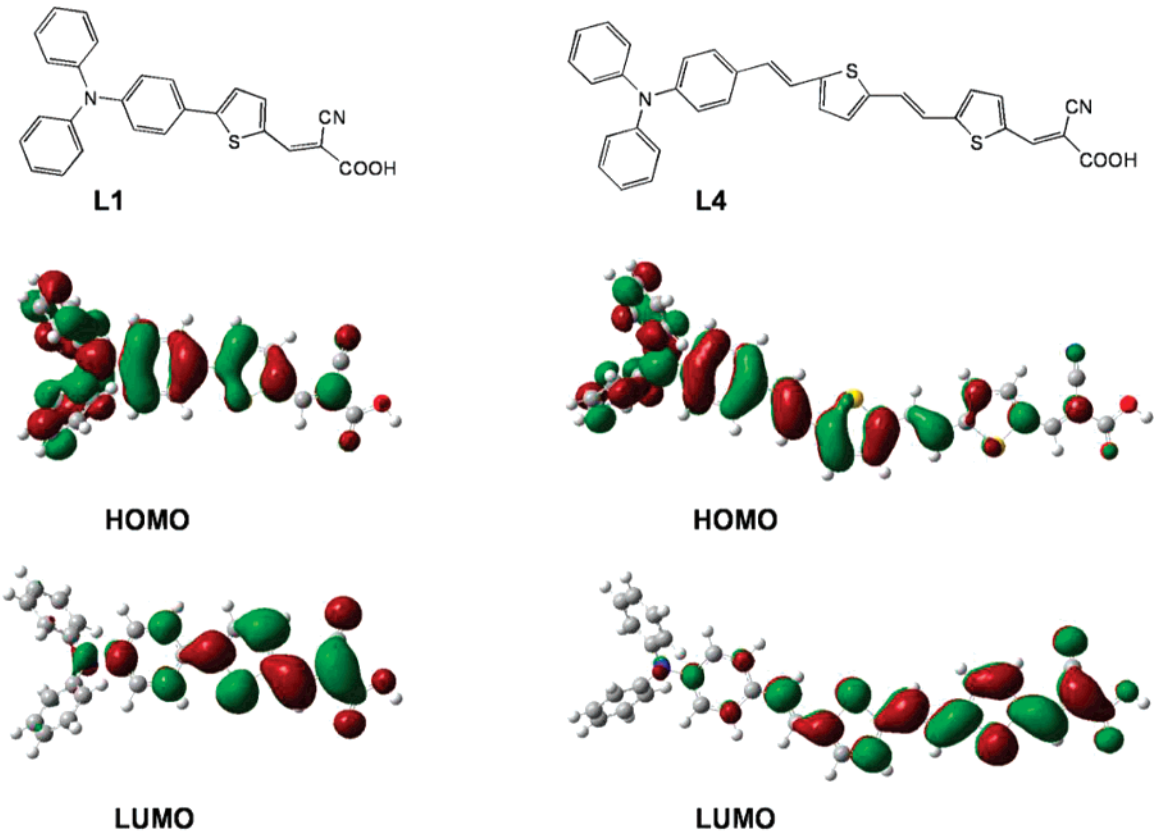

FIGURE 3. Computed isodensity surfaces of HOMO and LUMO orbitals of dyes **L1** and **L4**.

TABLE 2. Computed TDDFT Absorption Wavelengths (λ) and Oscillator Strengths for the First Electronic Transition

dye	λ_{max} [nm]	f
L0	401	0.81
L1	494	0.89
L2	537	1.08
L3	586	1.21
L4	621	1.34

photon-to-current conversion efficiency spectra are presented in Figure 4. The low-energy onsets of the IPCE spectra correlate well with E_{0-0} of the individual dyes. Solar cells based on **L0** and **L1** showed high IPCE (75%) but their spectra are not broad, resulting in lower overall efficiencies due to spectral limitations. Solar cells based on **L3** and **L4** show broad IPCEs in accordance to the broad absorption spectrum achieved by increasing the linker conjugation. The IPCE spectra is however lower over the whole spectral region compared to the other less conjugated dyes. The internal trend in IPCE between the dyes was observed independently of several parameters known to affect the dye load, i.e., the presence of deoxycholic acid in the dye bath, different dye concentrations, and variation in sensitization times.[24] Comparing the internal difference in dye load, the trend

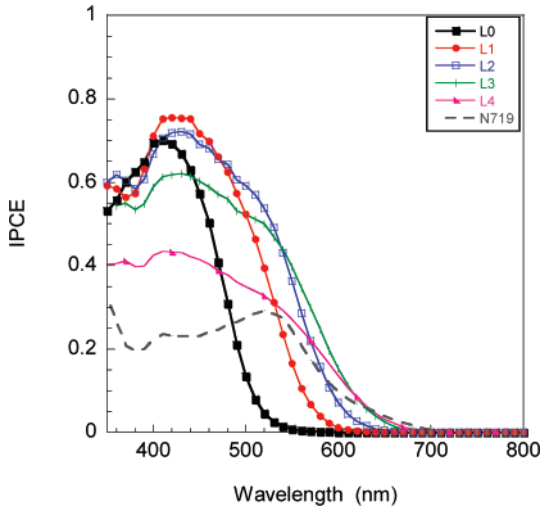

FIGURE 4. Spectra of monochromatic incident photon-to-current conversion efficiency (IPCE) for DSSC based on **L0**−**L4** and **N719**, respectively.

TABLE 3. Current and Voltage Characteristics of DSSCs (3 μm Thick WE) Based on the L0−L4[a]

dye	V_{oc} [mV]	η [%]	ff	J_{sc} [mA/cm^2]	dye load[b] [mmol/cm^3]	relative amount[c]
L0	735	1.55	0.73	2.89	227	1
L1	735	2.75	0.69	5.42	313	1.38
L2	710	3.08	0.68	6.42	264	1.16
L3	635	2.73	0.66	6.55	202	0.89
L4	580	1.70	0.64	4.56	133	0.59
N719	735	1.99	0.75	3.63		

[a] Photovoltaic performance under AM 1.5 irradiation of DSSCs based on **L0**−**L4** and **N719**, respectively, based on 0.6 M TBAI, 0.1 M LiI, 0.05 M I_2, 0.5 M 4-TBP electrolyte in acetonitrile. J_{sc} is the short-circuit photocurrent density; V_{oc} is the open-circuit voltage, ff is the fill factor, and η is the power conversion efficiency. [b] The dye loads are calculated from absorbance data of the sensitized TiO_2 electrodes. [c] The relative amount is calculated in reference to dye **L0**.

shows (see Table 3) that the amount of dye decreased as the dye size increases. Assuming a monolayer of the adsorbed dye onto the TiO_2, a larger dye will have a larger footprint (excluded volume) and hence result in a lower dye load. Considering the light harvesting efficiency, the relatively lower dye load of the larger dyes will be compensated by their higher extinction coefficients. The lower IPCE obtained for the longer **L3** and **L4** dyes could be caused by poor injection efficiency, possibly due to unfavorable binding or orientation of these dyes onto the TiO_2 surface. These results imply that the performance of the solar cells based on these dyes will in addition to the energetics also depend on the orientation, binding, and size of the dyes.

The photovoltaic performance of solar cells based on the different dyes **L0**−**L4** and 0.6 M TBAI, 0.1 M LiI, 0.05 M I_2, and 0.5 M 4-TBP electrolyte in acetonitrile under AM 1.5 illumination are summarized in Table 3. Light and dark current−voltage curves are shown in Figure 5, where a correlation between the linker length and the degree of generated dark current is observed. The dark current indicates the reaction with electrons in TiO_2 with electrolyte species where the properties of the semiconductor−dye interface will play a role. Concerning

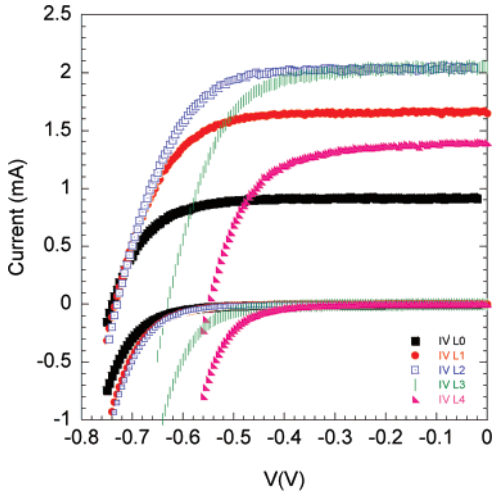

FIGURE 5. Light and dark current−voltage characteristics of DSSC based on **L0**−**L4**.

the observed trend in overall efficiencies; the spectrally comparable organic dyes, **L1**−**L3**, are performing better than **N719** due to higher extinction coefficients. DSSC based on **L0** have spectral limitations resulting in lower photocurrents as mentioned earlier, whereas **L4** showed a larger dark current and thus a higher degree of charge recombination mainly to the electrolyte.

In conclusion, chromophores **L0**−**L4** show satisfactory efficiencies on thin TiO_2 films (3 μm), and are therefore suitable for future solid-state devices. By increasing the π-conjugation of the linker, the HOMO and LUMO energy levels were tuned, which was further supported by electrochemistry and TDDFT calculations that show that these orbitals are distributed over the linker conjugation. Even though all dyes seem to fulfill the energetic criteria for DSSC the longer linker dyes showed pronounced losses. The longer linker conjugation gives increased spectral response but increases recombination of electrons to the triiodide, as supported by IV dark measurements. The lower IPCEs obtained for the longer **L3** and **L4** dyes could be due to binding and orientation problems affecting the injection efficiency. The reason could be due the specific nature of the dye (size/structure, orientation on the surface, chemical properties) and is under investigation at the moment. Solar cells based on **L2** yielded the highest efficiency (Table 3). The **L2** chromophore is thus showing the optimal properties in this study considering the energy levels and other parallel effects, as mentioned above, arising when varying the linker conjugation.

Experimental Section

General Procedure for Preparation of Solar Cells. TiO_2 nanocrystalline thin films were prepared by doctor blading on conducting glass substrates. The area of the TiO_2 film is 0.32 cm^2. The preparation of TiO_2 paste is described elsewhere.[25] The TiO_2 electrodes were sintered at 450 °C for 30 min. When the temperature decreased to 100 °C after the sintering the electrodes were immersed into 0.5 mM dye solutions and kept for 16 h at room temperature. The solvent was ethanol (99.5%) and acetonitrile (99.8%) for **N719** $(TBA)_2$-*cis*-$Ru(Hdcbpy)_2$-$(NCS)_2$ and **L** dyes, respectively. After the adsorption of the dyes, the electrode was rinsed with the same solvent. The electrodes were assembled with a counter electrode

(24) Wang, Z. S.; Cui, Y.; Dan-oh, Y.; Kasada, C.; Shinpo, A.; Hara, K. *J. Phys. Chem. C* **2007**, *111*, 7224.

(25) Wang, P.; Zakeeruddin, S. M.; Comte, P.; Charvet, R.; Humphry-Baker, R.; Grätzel, M. *J. Phys. Chem. B* **2003**, 107, 14336.

(thermally platinized) using a thermoplastic frame. Redox electrolyte was introduced through a hole drilled in the counter electrode that was sealed afterward. The electrolyte is 0.1 M LiI (99.9%), 0.6 M TBAI (98%), 0.05 M I_2 (99.9%), and 0.5 M 4-TBP (99%) in acetonitrile (99.8%). Prepared solar cells were characterized by current−voltage characteristics and incident photon-to-current conversion efficiency (IPCE). Current−voltage characteristics were carried out with a solar simulator (300 W xenon (ozone free)). IPCE measurements were carried out with a Xenon arc lamp (300 W), a 1/8 m monochromator, a source/meter, and a power meter with a 818-UV detector head.

General Synthetic Procedure. All reactions were carried out under N_2 with the use of standard inert atmosphere and Schlenk techniques. Dichloromethane (CH_2Cl_2), dimethylformamide (DMF), hexane, and tetrahydrofuran (THF) were dried by passing through a solvent column composed of activated alumina. ^{1}H and ^{13}C NMR spectra were recorded on 500 and 400 MHz instruments using the residual signals δ 7.26 and 77.0 ppm from $CDCl_3$, δ 2.50 and 39.4 ppm from d_6-DMSO, and δ 2.05, 29.84, and 206.26 ppm from d_6-acetone as internal references for ^{1}H and ^{13}C, respectively. HR-MS were performed by using a Q-Tof Micro mass spectrometry equipment with a Z-spray ionization source.

4-(Diphenylamino)phenylcyanoacrylic Acid (L0). A 50 mL acetonitrile solution of 4-diphenylaminobenzaldehyde (0.5 g, 1.83 mmol), cyanoacetic acid (0.19 g, 1.83 mmol), and piperidine (0.312 g, 3.66 mmol) was refluxed for 4 h under nitrogen atmosphere. Solvent removal by rotary evaporator followed by purification by extraction (petroleum ether and aq HCl (0.1 M)) yielded the product as a dark purple solid, **L0** (0.47 g, 73%): Mp 212.9−213.9 °C. IR (KBr) 1686, 2129, 2790. ^{1}H NMR (500 MHz, d_6-DMSO) δ 8.12 (s, 1H), 7.91 (d, J = 8.8 Hz, 2H), 7.43 (t, J = 7.7 Hz, 4H), 7.23 (m, 6H), 6.86 (d, J = 8.8 Hz, 2H). ^{13}C NMR (125 MHz, d_6-DMSO) δ 164.0, 153.0, 151.6, 145.1, 132.7, 129.9, 126.3, 125.5, 122.8, 118.0, 116.9, 98.0. HR-MS (TOF MS ES-) m/z 339.1142 [M − H$^+$] $^-$ calcd for $C_{22}H_{15}N_2O_2$ (M − H$^+$) 339.1134.

5-[2-(4-Diphenylaminophenyl)vinyl]thiophene.[17] The synthetic procedure and characterizations were presented in an earlier publication.[8]

5-[2-(4-Diphenylaminophenyl)vinyl]thiophene-2-carbaldehyde (1).[8] The synthetic procedure and characterizations were presented in an earlier publication.[8]

3-(5-(4-(Diphenylamino)styryl)thiophen-2-yl)-2-cyanoacrylic Acid (L2).[8] The synthetic procedure and characterizations were presented in an earlier publication.[8]

5-[2-(4-Diphenylaminostyryl)thiophene-2-ylvinyl]thiophene. 1 (0.170 g, 0.45 mmol) and *t*-BuOK (65 mg, 0.58 mmol) were dissolved in THF (22 mL) and the solution was stirred at ambient temperature under nitrogen atmosphere for 1 h. 2-Thienylmethyl triphenylphosphonium chloride (0.246 g, 10.2 mmol) was dissolved in THF and added dropwise to the solution. The reaction mixture was stirred for 1 h at ambient temperature, whereupon the mixture was heated to reflux for 5 h. The reaction mixture was allowed to cool to ambient temperature and a molar excess of water was added. The mixture was concentrated by rotary evaporator and the water phase was extracted with DCM. The organic phase was dried over $MgSO_4$, then filtered through a plug of silica gel (DCM), and a crude intermediate was obtained (0.2 g, 0.43 mmol). The crude product was used directly in the next step without further purification.

5-[2-(4-Diphenylaminostyryl)thiophene-2-ylvinyl]thiophene-2-carbaldehyde (2). 5-[2-(4-Diphenylaminostyryl)thiophene-2-ylvinyl]thiophene (50 mg, 0.11 mmol) was dissolved in THF (15 mL) and the solution was cooled to −78 °C under nitrogen atmosphere. *n*-Butyl lithium (0.2 mL, 1.6 M hexane solution) was added dropwise over 10 min and the mixture was stirred at −78 °C for 1 h. The mixture was allowed to warm to 0 °C and stirred for 30 min. The mixture was once again cooled to −78 °C and DMF (0.15 mL, 1.94 mmol) was added. The reaction mixture was allowed to warm to ambient temperature and stirred for 2 h. The reaction was quenched by the addition of aqueous HCl (10%, 50 mL) and extracted with DCM (3 × 30 mL). The combined organic extract was dried over anhydrous $MgSO_4$ and filtered. Solvent removal by rotary evaporation and column chromatography over silica gel with a DCM/petroleum ether mixture (75:25) was followed by cis-to-trans isomerization by reflux with I_2 (10 mg, 0.04 mmol) in toluene (40 mL). Solvent removal by rotary evaporation and column chromatography over silica gel using DCM/petroleum ether (1:1) yielded **2** as a red solid (34 mg, 64%): Mp 172.1−173.2 °C; IR (KBr) 1652. ^{1}H NMR (500 MHz, d_6-acetone) δ 9.90 (s, 1H), 7.88 (d, J = 3.9 Hz 1H), 7.49 (d, J = 8.6 Hz, 2H), 7.44 (d, J = 15.8 Hz, 1H), 7.36 (d, J = 3.9 Hz, 1H), 7.35−7.29 (m, 5H), 7.22 (d, J = 3.7 Hz, 1H), 7.17 (d, J = 15.8 Hz, 1H), 7.11−7.07 (m, 7H), 7.00−6.96 (m, 3H). ^{13}C NMR (125 MHz, d_6-acetone) δ 184.5, 153.3, 149.6, 149.4, 146.1, 143.7, 141.8, 139.9, 132.8, 131.7, 131.4, 130.8, 129.4, 129.1, 129.1, 127.6, 126.5, 126.5, 125.3, 124.8, 121.9. MS (APCI-Positive) m/z (+) 490.1 [M + H] $^+$.

5-[2-(4-Diphenylaminostyryl)thiophene-2-ylvinyl]thiophene-2-cyanoacrylic Acid (L4). A 50 mL acetonitrile solution of **2** (1 g, 2.6 mmol) and cyanoacetic acid (0.29 g, 3.4 mmol) was refluxed in the presence of piperidine (0.2 mmol, 17 mg) for 3 h under nitrogen atmosphere. Solvent removal by rotary evaporator followed by purification by column chromatography over silica gel with a DCM/methanol mixture (12:1) yielded the product as a dark purple solid, **L4** (78 mg, 72%): Mp 250.1−251.3 °C. IR (KBr) 1674. 2217. 3013. ^{1}H NMR (500 MHz, d_6-DMSO) δ 8.45 (s, 1H), 7.93 (d, J = 4.1 Hz, 1H), 7.49 (d, J = 8.7 Hz, 2H), 7.45−7.41 (m, 2H), 7.35−7.29 (m, 6H), 7.19 (d, J = 15.8 Hz, 1H), 7.14 (d, J = 3.9 Hz, 1H), 7.08 (t, J = 7.4 Hz, 2H), 7.05 (d, J = 7.4 Hz, 4H), 6.94−6.90 (m, 3H). ^{13}C NMR (125 MHz, d_6-DMSO) δ 163.6, 151.6, 147.0, 146.7, 146.2, 143.9, 141.3, 139.6, 134.0, 130.2, 130.3, 129.6, 128.6, 127.6, 127.5, 125.9, 124.3, 123.4, 122.4, 120.0, 119.8, 116.5, 97.5. HR-MS (TOF MS ES-) m/z 555.1219 [M − H$^+$] $^-$ calcd for $C_{34}H_{23}N_2O_2S_2$ (M − H$^+$) 555.1201.

5-[4-(Diphenylamino)phenyl]thiophene-2-carbaldehyde (3). To a solution of 4-bromo-*N*,*N*-diphenylaniline (200 mg 0.617 mmol) and $PdCl_2$(dppf) (51 mg 0.06 mmol) in dry toluene (2 mL) was added a solution of 5-formylthiophene-2-yl-2-boronic acid (192 mg, 1.23 mmol) and K_2CO_3 (426 mg, 3.10 mmol) in dry methanol (2 mL). The mixture was heated by microwave irradiation at 70 °C for 10 min. The reaction was quenched by the addition of water (30 mL) and extracted with DCM (3 × 30 mL). The combined organic extract was dried over anhydrous $NaSO_4$ and filtered. Solvent removal by rotary evaporation followed by column chromatography over silica gel with DCM/hexane (80/20) yielded a yellow oil (165 mg, 75%). IR (KBr) 1661. ^{1}H NMR (500 MHz, $CDCl_3$) δ 9.85 (s, 1 H), 7.69 (d, 1 H), 7.51 (d, 2 H), 7.29 (m, 5 H), 7.13 (d, 4H), 7.08 (t, 2H), 7.05 (d, 2H). ^{13}C NMR (125 MHz, $CDCl_3$) δ 182.6, 154.6, 149.1, 147.0, 141.3, 137.7, 129.5, 127.2, 126.1, 125.2, 123.9, 122.8, 122.3. HR-MS (TOF MS ESI) m/z 378.0895 [M + Na$^+$] calcd for $C_{23}H_{17}NNaOS$ (M + Na$^+$) 378.0929.

5-[4-(Diphenylamino)phenyl]thiophene-2-cyanoacrylic Acid (L1). A 5 mL acetonitrile solution of **3** (30 mg, 0.18 mmol), cyanoacetic acid (30 mg, 0.4 mmol), and piperidine (1.7 mg, 0.02 mmol) was refluxed for 4 h under nitrogen atmosphere. Purification by extraction (petroleum ether and aq HCl (0.1 M)) and filtration of the formed solid yielded the product as a dark red solid, **L1** (72 mg, 94%): Mp 239.0−240.2 °C. IR (KBr) 1683, 2216, 2816. ^{1}H NMR (500 MHz, d_6-DMSO) δ 8.46 (s, 1H), 7.99 (d, J = 4.10 Hz, 1H), 7.68 (d, J = 8.82 Hz, 2H), 7.63 (d, J = 4.10 Hz, 1H), 7.36 (t, J = 8.82 Hz, 4H), 7.14 (t, J = 7.56 Hz, 2H), 7.10 (d, J = 7.56 Hz, 4H), 6.97 (d, J = 8.82 Hz). ^{13}C NMR (125 MHz, d_6-DMSO) δ 163.7, 153.2, 148.6, 146.6, 146.3, 141.7, 133.4, 129.7, 127.4, 125.2, 125.0, 124.1, 123.9, 121.6, 116.5, 97.1. HR-MS (TOF MS ESI) m/z 445.0981 [M + Na$^+$] calcd for $C_{26}H_{18}N_2NaO_2S$ (M + Na$^+$) 445.0987.

5-[2-(4-Diphenylaminophenyl)thiophene-2-ylvinyl]thiophene. 2-Thienylmethyl triphenylphosphonium chloride (275 mg, 0.70 mmol) and *t*-BuOK (78 mg, 0.70 mmol) were dissolved in THF (15 mL) and the solution was stirred at ambient temperature under nitrogen atmosphere for 30 min. **3** (165 mg, 0.645 mmol) was dissolved in THF and added dropwise to the solution. The reaction mixture was stirred for 1 h at ambient temperature, whereupon the mixture was heated to reflux for 24 h. The reaction mixture was allowed to cool to ambient temperature and a molar excess of water was added. The water phase was extracted with DCM. The organic phase was dried over $NaSO_4$ and filtered and solvent was removed by rotary evaporation. Flash column chromatography over silica gel with petroleum ether/DCM (10/1) gave the crude thiophene (188 mg, 92%) as a yellow solid. The crude product was used in the next step. ^{1}H NMR (500 MHz, $CDCl_3$) δ 7.46 (d, J = 8.63 Hz, 1H), 7.27 (t, J = 8.56, 8.56 Hz, 4H), 7.18 (d, J = 5.02 Hz, 1H), 7.14−7.11 (m, 5H), 7.08−7.03 (m, 5H), 7.02 (d, J = 2.34 Hz, 2H), 6.99 (dd, J = 5.02, 3.60 Hz, 1H), 6.98 (d, J = 3.75 Hz, 1H). ^{13}C NMR (125 MHz, $CDCl_3$) δ 147.4, 147.4, 143.0, 142.5, 140.9, 129.3, 128.2, 127.7, 127.4, 126.379, 125.9, 124.6, 124.2, 123.5, 123.2, 122.7, 121.6, 120.5.

5-[2-(4-Diphenylaminophenyl)thiophene-2-ylvinyl]thiophene-2-carbaldehyde (4). 5-[2-(4-Diphenylaminophenyl)vinyl]thiophene (0.188 g, 0.431 mmol) was dissolved in THF (15 mL) and the solution was cooled to −78 °C under nitrogen atmosphere. *n*-Butyl lithium (0.35 mL, 1.6 M hexane solution) was added dropwise and the mixture was stirred at −78 °C for 30 min. The mixture was allowed to warm to ambient temperature and then stirred for 30 min. The mixture was once again cooled to −78 °C and DMF (0.05 mL, 0.65 mmol) was added. The reaction mixture was allowed to warm to ambient temperature and then stirred for 2 h. The reaction was quenched by the addition of aqueous HCl (10%, 100 mL) and extracted with DCM (3 × 30 mL). The combined organic extract was dried over anhydrous $NaSO_4$ and filtered. Solvent removal by rotary evaporation and column chromatography over silica gel with DCM/petroleum ether mixture (75:25) was followed by cis-to-trans isomerization by reflux with I_2 (5 mg, 0.02 mmol) in toluene (20 mL). Solvent removal by evaporation followed by column chromatography over silica gel with DCM/petroleum ether (1:1) yielded **4** as a light red oil (72 mg, 36%). IR (KBr) 1659. ^{1}H NMR (500 MHz, d_6-acetone) δ 9.90 (s, 1H), 7.87 (d, J = 3.91 Hz, 1H), 7.59 (d, J = 8.69 Hz, 2H), 7.44 (d, J = 15.89 Hz, 1H), 7.37−7.31 (m, 6H), 7.28 (d, J = 3.82 Hz, 1H), 7.18 (d, J = 15.90 Hz, 1H), 7.14−7.07 (m, 6H), 7.03 (d, J = 8.72 Hz, 2H). ^{13}C NMR (125 MHz, d_6-acetone) δ 184.4, 153.3, 149.7, 149.2, 146.5, 143.6, 141.8, 139.8, 132.0, 131.3, 129.5, 128.9, 128.4, 128.3, 127.5, 126.6, 126.5, 125.4, 125.3, 125.2, 124.8, 121.6. HR-MS (TOF MS ESI) m/z 486.0957 [M + Na^+] calcd for $C_{29}H_{21}NNaOS_2$ (M + Na^+) 486.0962.

5-[2-(4-Diphenylaminophenyl)thiophene-2-ylvinyl]thiophene-2-cyanoacrylic Acid (L3). A 10 mL acetonitrile solution of **4** (72 mg, 0.155 mmol), cyanoacetic acid (20 mg, 0.23 mmol), and piperidine (1.7 mg, 0.02 mmol) was refluxed for 4 h under nitrogen atmosphere. Purification by extraction (petroleoum ether and aq HCl (0.3 M)) and filtration of the formed solid yielded the product as a dark purple solid, **L3** (61 mg, 74%): Mp 213.5−214.6 °C. IR (KBr) 1681, 2214, 2922. ^{1}H NMR (500 MHz, d_6-DMSO) δ 8.44 (s, 1H), 7.92 (d, J = 4.11 Hz, 1H), 7.58 (d, J = 8.66 Hz, 2H), 7.47 (d, J = 15.84 Hz, 1H), 7.43 (d, J = 4.10 Hz, 1H), 7.41 (d, J = 3.83 Hz, 1H), 7.38 (d, J = 3.88 Hz, 1H), 7.34 (t, J = 7.90, 7.90 Hz, 4H), 7.23 (d, J = 15.90 Hz, 1H), 7.14−7.02 (m, 6H), 6.98 (d, J = 8.70 Hz, 2H). ^{13}C NMR (125 MHz, $CDCl_3$) δ 163.7, 151.6, 147.2, 146.6, 146.1, 144.1, 141.2, 139.6, 133.9, 130.8, 129.6, 127.3, 126.9, 126.4, 125.9, 124.4 124.3, 123.8, 123.5, 122.6, 119.5, 116.6, 97.6. HR-MS (TOF MS ESI) m/z 553.1015 [M + Na^+] calcd for $C_{32}H_{22}N_2NaO_2S_2$ (M + Na^+) 553.1020.

Acknowledgment. We acknowledge the Swedish Reasearch Council, Swedish Energy Agency, and the Knut and Alice Wallenberg foundation for financial support. The authors also thank Ms. Rong Zhang at Dalian University of Technology and Mr. Lien-Hoa Tran (Stockholms University) for the HR-MS measurements, and Dr. Xichuan Yang, Mr. Ruikui Chen, and Mr. Haining Tian (Dalian) for valuable discussions.

Supporting Information Available: ^{1}H NMR and ^{13}C NMR spectra for the new compounds described in this paper. This material is available free of charge via the Internet at http://pubs.acs.org.

JO701592X